Sulfur dioxide emissions from Peruvian copper smelters detected by the Ozone Monitoring Instrument

S. A. Carn,[1] A. J. Krueger,[1] N. A. Krotkov,[2] K. Yang,[2] and P. F. Levelt[3]

Received 6 December 2006; revised 20 March 2007; accepted 5 April 2007; published 1 May 2007.

[1] We report the first daily observations of sulfur dioxide (SO_2) emissions from copper smelters by a satellite-borne sensor - the Ozone Monitoring Instrument (OMI) on NASA's EOS/Aura spacecraft. Emissions from two Peruvian smelters (La Oroya and Ilo) were detected in up to 80% of OMI overpasses between September 2004 and June 2005. SO_2 production by each smelter in this period is assessed and compared with contemporaneous emissions from active volcanoes in Ecuador and southern Colombia. Annual SO_2 discharge from the Ilo smelter, La Oroya smelter, and volcanoes in 2004–2005 is estimated and amounts to $0.3^{+0.2}_{-0.1}$, 0.07 ± 0.03, and 1.2 ± 0.5 Tg, respectively. This study confirms OMI's potential as an effective tool for evaluation of anthropogenic and natural SO_2 emissions. Smelter plumes transport an array of toxic metals in addition to SO_2 and continued monitoring to mitigate health and environmental impacts is recommended.
Citation: Carn, S. A., A. J. Krueger, N. A. Krotkov, K. Yang, and P. F. Levelt (2007), Sulfur dioxide emissions from Peruvian copper smelters detected by the Ozone Monitoring Instrument, *Geophys. Res. Lett.*, *34*, L09801, doi:10.1029/2006GL029020.

1. Introduction

[2] Anthropogenic activities over the last century (mainly fossil fuel burning and metal smelting) have raised atmospheric SO_2 concentrations by up to 3 orders of magnitude [*Pham et al.*, 1996]. Of potentially greater significance is the concomitant increase in production of derived sulfate aerosol, which indirectly affects the climate system and water cycle by supplying cloud condensation nuclei, enhancing cloud albedo, and suppressing precipitation [*Twomey*, 1977; *Charlson et al.*, 1992; *Rosenfeld*, 2000]. An inventory of anthropogenic SO_2 source strengths is therefore a crucial component of global atmospheric models, but to date emissions from major source regions such as East Asia have typically been estimated using complex algorithms that rely on large input datasets, enumerating parameters such as fuel use and the removal efficiency of emission abatement systems [e.g., *Streets et al.*, 2003].

[3] As a viable alternative to these ''bottom-up'' estimates of emissions, the ultraviolet (UV) GOME and SCIAMACHY satellite sensors have demonstrated that anthropogenic SO_2 emissions can be detected from space [e.g., *Eisinger and Burrows*, 1998]. However, the efficacy of GOME and SCIAMACHY data for detailed studies of SO_2 emissions is restricted by poor spatial or temporal sampling. On July 15, 2004, NASA launched the Ozone Monitoring Instrument (OMI) as part of the EOS-Aura mission (http://aura.gsfc.nasa.gov). OMI has a unique combination of footprint size (13 × 24 km at nadir), spectral resolution (0.45 nm) and global contiguous coverage for space-based UV measurements of SO_2, surpassing the sensitivity of the Earth Probe Total Ozone Mapping Spectrometer (EP-TOMS), which could only detect anthropogenic SO_2 emissions when atmospheric loadings were exceptional [*Carn et al.*, 2004]. Using algorithms developed for retrieval of SO_2 from OMI, the noise level of SO_2 measurements has been reduced by an order of magnitude compared to the TOMS instruments [*Krotkov et al.*, 2006]. As we demonstrate here, these improvements permit detection of SO_2 discharge from specific industrial sources on a daily basis.

2. OMI Instrument and SO_2 Algorithm

[4] OMI is a hyperspectral UV/Visible spectrometer with a 2600 km swath for daily, contiguous global mapping of ozone and trace gases including SO_2, NO_2 and BrO. It was contributed to the 6-year Aura mission by the Royal Netherlands Meteorological Institute (KNMI) and the Netherlands Agency for Aerospace Programs (NIVR), in collaboration with the Finnish Meteorological Institute (FMI). Operational data flow from OMI began in September 2004. The Aura spacecraft is in a sun-synchronous orbit at 705 km altitude and crosses the equator at 1:45 pm ± 15 minutes local time each day (ascending node).

[5] Most OMI data products are currently produced using radiances at a subset of UV wavelengths calibrated with post-launch data. We have developed a scheme termed the Band Residual Difference (BRD) algorithm, which retrieves total column SO_2 using four OMI wavelengths situated at SO_2 band extrema between 310.8 and 314.4 nm [*Krotkov et al.*, 2006]. As described above, the BRD retrieval noise is an order of magnitude lower than achieved with EP-TOMS, permitting detection of weaker SO_2 sources and smaller SO_2 clouds with OMI. We have also developed time-averaging techniques which further improve the signal to noise ratio. All SO_2 data in this paper were produced using the BRD algorithm, the derivation of which is described by *Krotkov et al.* [2006].

[6] We caution that OMI SO_2 algorithms are subject to ongoing development and refinement, and that OMI SO_2 data have not yet been rigorously validated using correlative measurements. Retrieval of anthropogenic SO_2 in the planetary boundary layer (PBL) is particularly challenging due

[1] Joint Center for Earth Systems Technology, University of Maryland Baltimore County, Baltimore, Maryland, USA.
[2] Goddard Earth Sciences and Technology Center, University of Maryland Baltimore County, Baltimore, Maryland, USA.
[3] Royal Netherlands Meteorological Institute, De Bilt, Netherlands.

0094-8276/07/2006GL029020$05.00

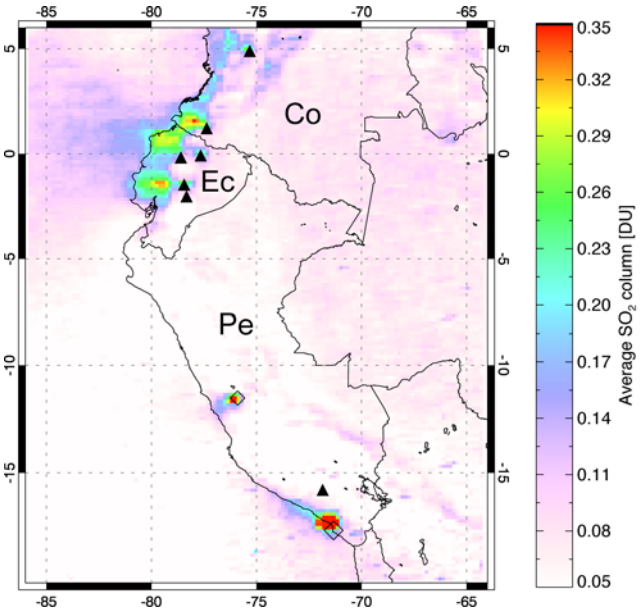

Figure 1. Average SO_2 column amounts measured by OMI over southern Colombia (Co), Ecuador (Ec), and Peru (Pe) between 1 September 2004 and 30 June 2005. Volcanoes (triangles), from north to south, are: Nevado del Ruiz, Galeras, Reventador, Guagua Pichincha, Tungurahua, Sangay, and Sabancaya. Peruvian copper smelters (diamonds; symbol size proportional to capacity) are located at La Oroya (11.53°S, 75.9°W) and Ilo (17.63°S, 71.33°W). Note the diffuse region of elevated SO_2 over the Pacific Ocean west of Ecuador and Colombia.

to reduced SO_2 sensitivity at low altitudes and variable degrees of concealment by clouds. The effects of aerosols are also not accounted for in the BRD algorithm. Although we endeavor to place realistic error bounds on the SO_2 amounts presented here, the emphasis is on the capabilities of OMI rather than the quantitative results. For the current status of OMI SO_2 algorithms and publicly released data, and associated documentation, the reader is referred to http://so2.umbc.edu/omi.

3. Sulfur Dioxide Emissions From Copper Smelters

[7] Copper smelting, involving extraction of copper from chalcopyrite ($CuFeS_2$), liberates large quantities of sulfur gases: ~2 tons of SO_2 are discharged in flue gases (which also contain CO_2 and NO_x) per ton of copper produced. Smelters have long been recognized as significant sources of SO_2 and other pollutants (including toxic heavy metals such as As, Cd, Cu, Pb, Se and Zn) [e.g., *Gidhagen et al.*, 2002]; for example, the environmental crisis associated with Ni-Cu smelting on NW Russia's Kola Peninsula is well known [*Simonetti et al.*, 2004]. Most polluting smelters are now situated in developing countries, where modern sulfur capture technology may be unavailable or unaffordable. Approximately 50% of smelters capture <84% of emitted SO_2, whilst 10% capture none at all [*Boon et al.*, 2001]. Most of the latter are situated in Australasia, South America, Africa and China.

[8] Analysis of early OMI SO_2 data revealed two persistent sources of SO_2 in Peru that did not correspond to the locations of active volcanoes (Figure 1). These were subsequently identified as copper smelters situated in Ilo (at sea level in southern Peru; owned by the Southern Peru Copper Company) and La Oroya (112 miles north-east of Lima; alt. 12,385 ft; operated by The Doe Run Company, La Oroya, Peru, http://www.doerun.com/whatwedo/laOroya.aspx). Annual capacities of these smelters in 2002 were reportedly 300 and 80 thousand metric tons, respectively [*Feliciano and González*, 2003], making Ilo one of the ten largest copper smelters in the world. This output would yield annual SO_2 emissions of 0.6 and 0.16 Tg, respectively, assuming 2 tons of SO_2 emitted per ton of copper produced, operation at maximum capacity, and no SO_2 capture. *Boon et al.* [2001] report annual SO_2 emissions amounting to 0.42 Tg from the Ilo smelter (several times larger than the total output of many European nations), which at the time captured 30% of its SO_2 yield for sulfuric acid production. These amounts are commensurate with SO_2 production reported for these smelters in the Global Emissions Inventory Activity (GEIA) database for 1985 (http://www.geiacenter.org). *Boon et al.* [2001] also note that a 250 MW coal-fired power plant is located 25 km south of Ilo, although the SO_2 emissions are significantly lower than those from the smelter.

[9] Both Peruvian copper smelters are implicated in poor local air quality and health crises and are aiming to reduce pollution by increasing SO_2 capture [*Boon et al.*, 2001; *Centers for Disease Control*, 2005]. Modernization of the Ilo smelter was scheduled for completion in 2006 and will result in capture of 93% of SO_2 emissions [*Boon et al.*, 2001]. As a demonstration of OMI's capabilities, we report here OMI measurements of SO_2 burdens over Peruvian smelters from September 2004–June 2005, and compare them with contemporaneous SO_2 emissions from active volcanoes in Ecuador and S. Colombia.

4. OMI SO_2 Data Analysis

[10] We calculated daily mean SO_2 burdens measured by OMI over three regions for each month (Table 1). Regions were delineated according to the maximum extent of SO_2 plumes observed from each source in a single day of OMI data. BRD algorithm SO_2 retrievals assumed an SO_2 layer altitude of 5 km for the La Oroya smelter and the high-altitude volcanoes of Ecuador/S. Colombia, and <3 km (PBL) for the coastal Ilo smelter. Total SO_2 amounts in Table 1 were calculated by summing all the SO_2 retrieved in the region during each month and applying a background correction using an adjacent box of similar dimensions containing no significant SO_2 sources. Mean burdens were then derived in two ways (M_D and M_{Obs}; Table 1); M_{Obs} (based on observed SO_2 plumes) being an attempt to compensate for inevitable masking of SO_2 by cloud on certain days. Figure 2 depicts raw daily SO_2 burdens for each region without a background correction.

[11] The map in Figure 1 depicts the long-term average distribution of SO_2 measured by OMI in 2004–2005. Dispersal of SO_2 from La Oroya occurs predominantly to the southwest (towards Lima), whilst the SO_2 plume from Ilo, clearly the stronger source, typically hugs the coastline

Table 1. Mean Daily SO_2 Burdens Measured by OMI, September 2004–June 2005[a]

		Ecuador, Southern Colombia[b]				Ilo Smelter[b]				La Oroya Smelter[b]			
	Data[d]	Total[e]	M_D[d]	Obs[f]	M_{Obs}[f]	Total	M_D	Obs	M_{Obs}	Total	M_D	Obs	M_{Obs}
Sep 04[c]	15	24	1.59	11	2.17	15	0.98	12	1.23	3.1	0.21	10	0.31
Oct 04	30	40	1.35	19	2.12	32	1.07	26	1.24	6.7	0.22	23	0.29
Nov 04[c]	17	26	1.55	14	1.88	16	0.93	16	0.98	2.4	0.14	8	0.30
Dec 04[c]	29	52	1.80	23	2.27	20	0.69	24	0.83	3.3	0.11	15	0.22
Jan 05	30	56	1.85	22	2.52	15	0.49	22	0.67	3.0	0.10	22	0.14
Feb 05	27	62	2.30	19	3.28	14	0.53	22	0.65	1.3	0.05	10	0.13
Mar 05	30	26	0.87	11	2.37	18	0.60	25	0.72	2.2	0.07	21	0.10
Apr 05	29	32	1.10	6	5.33	12	0.42	22	0.55	2.4	0.08	17	0.14
May 05	30	68	2.27	16	4.25	13	0.45	23	0.58	3.6	0.12	20	0.18
Jun 05	29	121	4.18	21	5.78	15	0.51	23	0.65	6.4	0.22	23	0.28
TOTAL	266	508		162		170		215		34		169	

[a]Unit of measure for mean daily SO_2 burdens is Gg.
[b]Ecuador and southern Colombia, lat 3°N–5°S, lon 84°–76°W; Ilo, lat 15°–18.5°S, lon 76°–70.5°W; La Oroya, lat 10.5°–14°S, lon 79°–75°W.
[c]Data gaps occur from 1–5 Sep, 16–23 Sep, and 19 Nov–1 Dec 2004 inclusive. OMI is also in a special zoom observation mode on 1 day per month; these data are not currently used for SO_2 measurements.
[d]Number of days with OMI measurements per month. M_D is the mean daily SO_2 burden calculated using this figure.
[e]Total measured SO_2 emissions per month.
[f]Number of days with observed SO_2 plumes per month (for Ecuador and southern Colombia, simultaneous SO_2 plumes from >1 volcano were counted as a single observation). M_{Obs} is the mean daily SO_2 burden calculated using this figure.

northwest of the smelter and is traceable for ~300 km. No other strong point sources of SO_2 are apparent in Peru.

[12] SO_2 emissions from active volcanoes in Ecuador and Colombia are clearly visible in Figure 1. In the timeframe studied, Reventador and Tungurahua (Ecuador) and Galeras (Colombia) were the most active (e.g., see archived volcanic ash advisories issued for the region at http://www.ssd.noaa.gov/VAAC/messages.html). Note that although a small SO_2 anomaly appears to be associated with Nevado del Ruiz volcano (Colombia; Figure 1), this was not included in the SO_2 burden calculations given in Table 1 and Figure 2. A spike in the SO_2 burden over Ecuador/S. Colombia in mid-May (Figure 2) was due to the transit of an SO_2 cloud from an eruption of Fernandina (Galapagos Is) across the region. We cannot rule out a contribution to the SO_2 burden measured over Ecuador/S. Colombia from anthropogenic sources along the coastal plain, and there is possible evidence for such sources in the OMI data (Figure 1). However, the 1985 GEIA database indicates that these sources would contribute on the order of 0.01 Gg/day or less of SO_2, which is <1% of the total amounts measured by OMI (Table 1). OMI does not currently provide information on the vertical distribution of SO_2 and therefore cannot

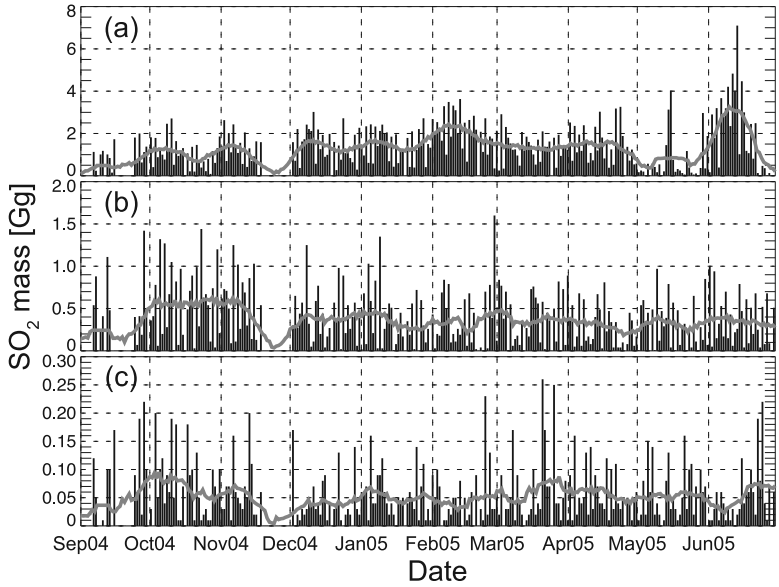

Figure 2. Daily SO_2 burdens (vertical bars) measured by OMI over (a) Ecuador and southern Colombia, (b) Ilo, and (c) La Oroya. Some of the variability in these burdens is due to cross-track variations in OMI ground pixel size, from 13 × 24 km at nadir to an estimated 41 × 140 km at the swath edge. Thus, sensitivity to SO_2 is reduced when the target is located at the swath edge. A 14-day centered moving average (grey curve) shows the general trend in the data. See Table 1 for the bounds of each region. Note the OMI data gaps listed in Table 1 (which produce false minima in the smoothed data), and varying scale on the ordinate.

distinguish between volcanic and anthropogenic SO_2 where both occur in close proximity.

[13] We have also assessed the potential error on PBL SO_2 columns due to aerosol effects, since these are not accounted for in the BRD algorithm. A realistic aerosol model was derived using parameters obtained from the AERONET (Aerosol Robotic Network, http://aeronet.gsfc.nasa.gov) site closest to the Ilo smelter (Arica, N. Chile; 18.47°S, 70.31°W). Radiative transfer simulations incorporating this model indicate that aerosol effects are minor for measurements at or near-nadir, but that the BRD algorithm may underestimate PBL SO_2 columns by a factor of 2 for extreme off-nadir viewing geometry, which occurs approximately once every 6 days. This result holds for model aerosol vertical distributions with half-widths of 1 km (aerosol closer to the ground) and 2 km (larger vertical extent of aerosol). Errors on the Ilo SO_2 emissions reported below reflect this tendency to underestimate PBL SO_2 amounts; the effect is less significant for SO_2 located at higher altitudes. We stress that these conclusions are particular to the Ilo site, and that aerosol parameters and vertical profiles of SO_2 and aerosols specific to each location are needed to assess these effects more accurately.

5. Discussion

[14] The Ilo smelter was the most persistent SO_2 source in the 10-month period studied, with emissions detected in ~80% of OMI observations (Table 1). In terms of source strength, the volcanoes of Ecuador/S. Colombia were dominant (particularly during a period of elevated activity at Reventador in June 2005; Figure 2), followed by Ilo and La Oroya, with mean M_{Obs} ($\pm 1\sigma$) of 3.2 ± 1.4, $0.8^{+0.4}_{-0.25}$ and 0.2 ± 0.08 Gg, respectively. The volcanic signal showed most variability, whilst SO_2 burdens over Ilo were the most consistent.

[15] Based on average observed burdens, and assuming an SO_2 lifetime of 1 day, annual SO_2 discharge from the Ilo and La Oroya smelters is currently on the order of $0.3^{+0.2}_{-0.1}$ and 0.07 ± 0.03 Tg, which for Ilo compares well with published data [*Boon et al.*, 2001], given the higher uncertainty on PBL SO_2 columns. The annual volcanic flux for Ecuador and S. Colombia amounts to 1.2 ± 0.5 Tg. We caution that conversion rates lower than 100% SO_2 day^{-1} would reduce these values. We note a significant decline in daily SO_2 burdens at the Ilo smelter, from ~1 Gg or more in September–November 2004 to an average of ~0.6 Gg from January 2005 onwards (Table 1; Figure 2). Although we cannot exclude factors such as a reduction in smelter operating capacity or a change in the aerosol regime at this stage, this may reflect ongoing modernization of the smelter and increased SO_2 capture. SO_2 burdens over the La Oroya smelter were ostensibly lower between December 2004 and April 2005 (Table 1), but this coincides with the Andean wet season, and we therefore attribute this trend to increased cloudiness and/or wet deposition of SO_2 in this period. The Peruvian coast around Ilo is, in contrast, rather arid year-round.

[16] Uncertainty on actual SO_2 emissions arises from inadequate constraints on SO_2 conversion rates and their temporal variability. Concentrations of SO_2 near the smelters vary diurnally, peaking at night or in the morning at both plants [*Boon et al.*, 2001; *Dirección General de Salud Ambiental*, 1999]. This is probably a result of the temperature dependence of the rate constant for the SO_2 (g) to sulfate conversion [*Eatough et al.*, 1994], and the exhaustion of oxidants (primarily the OH radical, derived from photolysis of O_3) at night. Studies of copper smelter plumes document gas-phase homogeneous SO_2 conversion rates of ~1–8% hr^{-1}, peaking in hot (~30°C), sunny conditions [*Eatough et al.*, 1982], which are similar to reported rates in power plant plumes, suggesting that the trace metal content of smelter emissions has no appreciable catalytic effect [*Hewitt*, 2001].

[17] Aqueous-phase conversion of SO_2 to sulfate (e.g., plumes entrained into cloud or fog) can proceed at rates up to 100% hr^{-1} but is also dependent on the availability of oxidants (principally H_2O_2 and O_3) [*Eatough et al.*, 1984; *Eatough et al.*, 1994]. Fog (*garua*) affects the coast of Peru from May – November, but we see no clear artifacts in the Ilo data (Table 1), possibly because the plume is not emitted into fog or because the supply of the necessary oxidants is inadequate. Given the anisotropic dispersal of the emissions (Figure 1) the supply of oxidants in the plume might become limiting at times, which could explain the surprisingly large extent of the SO_2 plume from Ilo in Figure 1. The potential impacts of Ilo smelter pollution on fog acidity warrant further study, since in this arid region the water supply is augmented by harvesting (condensing) fog.

[18] The early afternoon OMI overpass therefore likely coincides with peak SO_2 conversion rates and minimum ambient SO_2 concentrations, but the SO_2 plume mapped in an OMI snapshot is the cumulative product of emission, transport and conversion over a 24-hour period. Conversion rates depend on temperature, relative humidity, droplet size, oxidant abundance, meteorology and the relative significance of gas-phase and aqueous-phase reactions [*Eatough et al.*, 1994]. Constant conversion at 8% hr^{-1} would result in a SO_2 lifetime of <1 day and a potential underestimate of SO_2 emissions by OMI, whereas removal of 1% SO_2 hr^{-1} in daylight could produce daily residuals of over 80% of the previous day's discharge, and overestimated emissions. The reality probably falls between these extremes, but would require a complex model for resolution and is beyond the scope of this paper. We also note that any diurnal variation in smelter emissions (for which data are unavailable) would not be captured by the OMI measurements, particularly if the SO_2 lifetime were <1 day. Emissions might be significantly underestimated if the smelters only operate at night.

[19] Although the smelter emissions are undoubtedly significant, regional average SO_2 column amounts (Figure 1) highlight the more widespread impact of volcanic emissions in 2004–2005. A diffuse zone of elevated SO_2 can be seen extending west from the region across the Pacific (Figure 1), and most likely reflects the higher altitude and source strength of the volcanic emissions. Continued analysis of OMI SO_2 data throughout the Aura mission will establish whether this is typical, or a result of above-average levels of volcanic unrest in 2004–2005.

6. Conclusions

[20] We have demonstrated that the UV OMI sensor on Aura can detect daily tropospheric emissions from anthro-

pogenic and natural sources of SO_2. Due to its relatively short tropospheric residence time [*Eatough et al.*, 1994], SO_2 is not a significant greenhouse gas, but it is easier to measure than longer-lived species such as CO_2, CH_4 and N_2O and hence can be used to pinpoint major sources of pollution and quantify source strengths.

[21] Numerous other anthropogenic SO_2 sources have been sensed by OMI. Smelter and power plant pollution in Chile, Eastern Europe, Russia, China and Uzbekistan has also been detected. The recognized health impacts of the array of toxic metals released in smelter plumes warrant increased efforts to monitor and map such emissions, though *Boon et al.* [2001] note that access to environmental monitoring data is often difficult in Latin America, Asia and Africa. Space-based monitoring of emissions with instruments such as OMI offers an economical solution to this problem.

[22] An irrefutable contribution of anthropogenic activities to global warming over the last century is now widely acknowledged [*Intergovernmental Panel on Climate Change (IPCC)*, 2001]. Quantification of the negative forcing by atmospheric sulfate aerosol, plus indirect aerosol effects, is a critical, yet poorly constrained, aspect of climate models [*IPCC*, 2001]. Accurate mapping of the spatial and temporal variability of SO_2 emissions using OMI will therefore contribute to improved modeling of the climate system. OMI measurements could also facilitate mitigation of health and environmental impacts of SO_2 and sulfate aerosol (e.g., visibility impairment, acid rain) close to sources.

[23] **Acknowledgments.** We acknowledge the NASA Science Mission Directorate's Earth-Sun System Division for funding of OMI SO_2 product development and analysis. Data used in this paper were produced by NASA in collaboration with the Royal Dutch Meteorological Institute (KNMI) in the Netherlands. The OMI project is managed by KNMI and the Netherlands Agency for Aerospace Programs (NIVR). We thank Brent Holben for his effort in establishing and maintaining the Arica AERONET site, and two reviewers for insightful comments on the paper.

References

Boon, R. G. J., A. Alexaki, and E. H. Becerra (2001), The Ilo Clean Air Project: A local response to industrial pollution control in Peru, *Environ. Urbanization*, *13*(2), 215–232.

Carn, S. A., A. J. Krueger, N. A. Krotkov, and M. A. Gray (2004), Fire at Iraqi sulfur plant emits SO_2 clouds detected by Earth Probe TOMS, *Geophys. Res. Lett.*, *31*, L19105, doi:10.1029/2004GL020719.

Centers for Disease Control (2005), Development of an integrated intervention plan to reduce exposure to lead and other contaminants in the mining center of La Oroya, Perú, Cent. for Disease Control and Prev. Natl. Cent. for Environ. Health, Atlanta, Ga., http://www.cdc.gov/nceh/ehs/Docs/la_oroya_report.pdf.

Charlson, R. J., S. E. Schwartz, J. M. Hales, R. D. Cess, J. A. Coakley, J. E. Hansen, and D. J. Hofmann (1992), Climate forcing by anthropogenic aerosols, *Science*, *255*, 423–430.

Dirección General de Salud Ambiental (1999), Evaluacion de la calidad del aire en el distrito de La Oroya-Junin, DIGESA, Lima, Perú, http://www.digesa.sld.pe/aire/pdf/puntual/oroya1999.pdf.

Eatough, D. J., et al. (1982), Sulfur chemistry in a copper smelter plume, *Atmos. Environ.*, *16*, 1001–1015.

Eatough, D. J., R. J. Arthur, N. L. Eatough, M. W. Hill, N. F. Mangelson, B. E. Richter, and L. D. Hansen (1984), Rapid conversion of SO_2 (g) to sulfate in a fog bank, *Environ. Sci. Technol.*, *18*(11), 855–859.

Eatough, D. J., F. M. Caka, and R. J. Farber (1994), The conversion of SO_2 to sulfate in the atmosphere, *Isr. J. Chem.*, *34*(3–4), 301–314.

Eisinger, M., and J. P. Burrows (1998), Tropospheric sulfur dioxide observed by the ERS-2 GOME instrument, *Geophys. Res. Lett.*, *25*, 4177–4180.

Feliciano, C. S. L., and E. González (2003), Map and table of world copper smelters, *U.S. Geol. Surv. Open File Rep.*, *03-075*, http://pubs.usgs.gov/of/2003/of03-075/index.html.

Gidhagen, L., H. Kahelin, P. Schmidt-Thomé, and C. Johansson (2002), Anthropogenic and natural levels of arsenic in PM10 in central and northern Chile, *Atmos. Environ.*, *36*, 3803–3817.

Hewitt, C. N. (2001), The atmospheric chemistry of sulphur and nitrogen in power station plumes, *Atmos. Environ.*, *35*, 1155–1170.

Intergovernmental Panel on Climate Change (IPCC) (2001), *Climate Change 2001: The Scientific Basis*, *Contribution of Working Group I to the Third Assessment Report of the Intergovernmental Panel on Climate Change*, edited by J. T. Houghton et al., 944 pp., Cambridge Univ. Press, New York, http://www.grida.no/climate/ipcc_tar/wg1/index.htm.

Krotkov, N. A., S. A. Carn, A. J. Krueger, P. K. Bhartia, and K. Yang (2006), Band Residual Difference algorithm for retrieval of SO_2 from the Aura Ozone Monitoring Instrument (OMI), *IEEE Trans. Geosci. Remote Sens.*, *44*(5), 1259–1266, doi:10.1109/TGRS.2005.861932.

Pham, M., J.-F. Müller, G. P. Brasseur, C. Granier, and G. Mégie (1996), A 3D model study of the global sulphur cycle: Contributions of anthropogenic and biogenic sources, *Atmos. Environ.*, *30*, 1815–1822.

Rosenfeld, D. (2000), Suppression of rain and snow by urban and industrial air pollution, *Science*, *287*, 1793–1796.

Simonetti, A., C. Gariépy, C. M. Banic, R. Tanabe, and H. K. Wong (2004), Pb isotopic investigation of aircraft-sampled emissions from the Horne smelter (Rouyn, Québec): Implications for atmospheric pollution in northeastern North America, *Geochim. Cosmochim. Acta*, *68*(16), 3285–3294, doi:10.1016/j.gca.2004.02.008.

Streets, D. G., et al. (2003), An inventory of gaseous and primary aerosol emissions in Asia in the year 2000, *J. Geophys. Res.*, *108*(D21), 8809, doi:10.1029/2002JD003093.

Twomey, S. A. (1977), The influence of pollution on the shortwave albedo of clouds, *J. Atmos. Sci.*, *34*, 1149–1152.

S. A. Carn and A. J. Krueger, Joint Center for Earth Systems Technology, University of Maryland Baltimore County, Baltimore, MD 21250, USA. (scarn@umbc.edu)

N. A. Krotkov and K. Yang, Goddard Earth Sciences and Technology Center, University of Maryland Baltimore County, Baltimore, MD 21250, USA.

P. F. Levelt, Royal Netherlands Meteorological Institute, NL-3730 AE De Bilt, Netherlands.